Computers and Concrete, *Vol. 14, No. 6 (2014) 745-765*
DOI: http://dx.doi.org/10.12989/cac.2014.14.6.745

Finite element model updating effect on the structural behavior of long span concrete highway bridges

A.C. Altunisik* and A. Bayraktar

Department of Civil Engineering, Karadeniz Technical University, Trabzon, Turkey

(*Received May 6, 2014, Revised July 31, 2014, Accepted August 31, 2014*)

Abstract. In this paper, it is aimed to determine the finite element model updating effects on the structural behavior of long span concrete highway bridges. Birecik Highway Bridge located on the 81stkm of Şanlıurfa-Gaziantep state highway over Fırat River in Turkey is selected as a case study. The bridge consist of fourteen spans, each of span has a nearly 26m. The total bridge length is 380m and width of bridge is 10m. Firstly, the analytical dynamic characteristics such as natural frequencies and mode shapes are attained from finite element analyses using SAP2000 program. After, experimental dynamic characteristics are specified from field investigations using Operational Modal Analysis method. Enhanced Frequency Domain Decomposition method in the frequency domain is used to extract the dynamic characteristics such as natural frequencies, mode shapes and damping ratios. Analytically and experimentally identified dynamic characteristics are compared with each other and finite element model of the bridge is updated to reduce the differences by changing of some uncertain parameters such as section properties, damages, boundary conditions and material properties. At the end of the study, structural performance of the highway bridge is determined under dead load, live load, and dynamic loads before and after model updating to specify the updating effect. Displacements, internal forces and stresses are used as comparison parameters. From the study, it is seen that the ambient vibration measurements are enough to identify the most significant modes of long span highway bridges. Maximum differences between the natural frequencies are reduced averagely from %46.7 to %2.39 by model updating. A good harmony is found between mode shapes after finite element model updating. It is demonstrated that finite element model updating has an important effect on the structural performance of the arch type long span highway bridge. Maximum displacements, shear forces, bending moments and compressive stresses are reduced %28.6, %21.0, %19.22, and %33.3-20.0, respectively.

Keywords: dynamic characteristics; enhanced frequency domain decomposition; finite element model updating; long span concrete highway bridge; operational modal analysis

1. Introduction

Birecik arch type long span highway bridge located on the 81stkm of Şanlıurfa-Gaziantep state highway over Fırat River in Turkey. Because of the fact that the bridge is the sole in this part of Fırat, it has a major logistical importance. The construction of the bridge was started in June 1951 and the bridge was opened the traffic in April 1956. The bridge is the longest concrete highway

*Corresponding author, Associate Professor, E-mail: ahmetcan8284@hotmail.com

http://www.techno-press.org/?journal=cac&subpage=8 ISSN: 1598-8198 (Print), 1598-818X (Online)

a) General appearance

b) Construction joints

c) Support types

Fig. 1 Some views of general appearance, joints and support types of theBirecik long span concrete highway bridge

bridge of Turkey considering the construction date. The bridge consist of fourteen spans, each of span has a nearly 26m. The total bridge length is 380m and width of bridge is 10m. The beams have rigid connectivity at the middle spans and side supports. Three expansion joints are placement symmetrically to eliminate the extra external forces. Columns, beams, decks and foundations were constructed as reinforced concrete. Some views of general appearance, joints and support types of the bridge are given in Fig. 1.

Among all types of civil engineering structures, long span highway bridges attract the greatest interest for studies of structural performance by the literature (Brownjohn *et al*. 2010). To succeed this aim, experimental field testing under ambient conditions is consistently increasing in popularity nowadays. Finite element models must be pictured of current behavior of this type of the structures as soon as possible to determine the structural earthquake responses more exactly. But it is usual to make simplifying assumptions in the development of finite element models. Because, the finite element models are constructed on the basis of highly idealized engineering blueprints and designs that may or may not truly represent all the physical aspects of an actual structure. When experimental measurement tests are performed to validate the analytical model, do not coincide with the expected results from the finite element model. These discrepancies originate from the uncertainties in simplifying assumptions of structural geometry, materials, as well as inaccurate boundary conditions (Bayraktar *et al*. 2010). So, analytical dynamic characteristics must be approved by experimental techniques and finite element model of the structures must be updated to eliminate the differences.

There are many studies in the literature about the finite element model updating of bridges. Jaishi and Ren (2006) studied about the damage detection by finite element model updating using modal flexibility residual. Jaishi *et al*. (2007) carried out the finite element model calibration of concrete filled steel tubular arch bridge under operational condition using modal flexibility. Schlune *et al*. (2009) performed the improved bridge evaluation through finite element model updating using static and dynamic measurements. Weng *et al*. (2011) presented to substructure based approach to finite element model updating procedures of Balla Balla River Bridge with division formation of eleven substructures. Magalhaes *et al*. (2012) realized the ambient and free vibration tests of the Millau Viaduct. The viaduct is the tallest vehicular bridge in the world, with the top of a pylon rising at 343m above the river level, and due to its total length of 2460m. Ubertini *et al*. (2013) practiced about the automated modal identification of engineering structures in operational conditions. Also, this procedure is applied to bridge structures as a case study. Mosavi *et al*. (2013) calibrated a high-fidelity finite element model of a highway bridge using a multi-variable sensitivity-based optimization approach. It can be seen from the literature that there is no enough studies about finite element mdel updating effects on the earthquake behavior of long span concrete highway bridges under dead load, live load and dynamic loads.

The objective of this study is to determine the finite element model updating effect on the earthquake behavior of long span concrete highway bridge. Birecik highway bridge located on the Şanlıurfa-Gaziantep state highway is chosen as an application. The initial finite element model of the bridge is modelled using SAP2000. Operational Modal Analysis method is used to extract dynamic characteristics. Finite element model of the bridge is updated to reduce the differences by changing of some uncertain parameters such as section properties, damages, boundary conditions and material properties. Earthquake behavior of the highway bridge is determined under dead load, live load, and dynamic loads before and after finite element model updating to specify the updating effect.

2. Formulation

Ambient excitation does not lend itself to Frequency Response Function (FRFs) or Impulse Response Function (IRFs) calculations because the input force is not measured in an ambient vibration test. Therefore, a modal identification procedure will need to base itself on output-only data (Ren *et al*. 2004). There are several modal parameter identification methods available. These methods are developed by improvements in computing capacity and signal processing procedures. In this study, Enhanced Frequency Domain Decomposition (EFDD) in the frequency domain is used for modal parameter extraction. The background and formulation of the EFDD can be available from the literature (Felber 1993; Peeters 2000; Bendat and Piersol 2004; Jacobsen *et al*. 2006; Rainieri *et al*. 2007).

3. Finite element analysis

3D finite element model of the bridge is modelled using building survey drawings by SAP2000 software (SAP2000, 1998). Beams are modeled by frame elements having three translational DOFs and three rotational DOFs at each node. Deck and side walls are modeled by shell elements. Also, columns are modelled by solid elements. Expansion joints are modeled using restricted boundary conditions using very rigidity springs. To reflect the variable sections of the deck beams both longitudinal and transverse directions, individual lines are modelled and insertion point option with rigid bodies are considered. The initial material propertied are determined by experimental studies. Material and soil properties obtained from the laboratory tests are given in Table 1.

To determine the structural behavior of the bridge beams as soon as possible and to compare the analytical results with experimental results for the aim of model updating, experimental measurements were separately conducted on the each bridge beams. At the end of the experimental measurements, it is seen that frequency span of each bridge beam span were parallel to each other. For this reason, initial finite element model of the bridge was constituted for one bridge beam span. Improvements to be made at the beams according to the experimental measurements applied to other bridge beams and all bridge model was obtained. The column-foundation interaction points were modeled using very rigid springs in the initial finite element model. Expansion joints were modeled using spring and link elements which have longitudinal, transverse and vertical displacements stiffness. Fig. 2 shows three dimensional initial finite element model of the bridge arch.

Table 1 Material properties considered in finite element analyses

Elements	Material Properties		
	Modulus of Elasticity (N/m^2)	*Poisson Ratio* (-)	*Density* (kg/m^3)
Column	3.0E10	0.2	2450
Beam	3.0E10	0.2	2450
Deck	3.0E10	0.2	2450
Foundation	3.2E10	0.2	2450
Rebar	2.0E11	0.3	7850

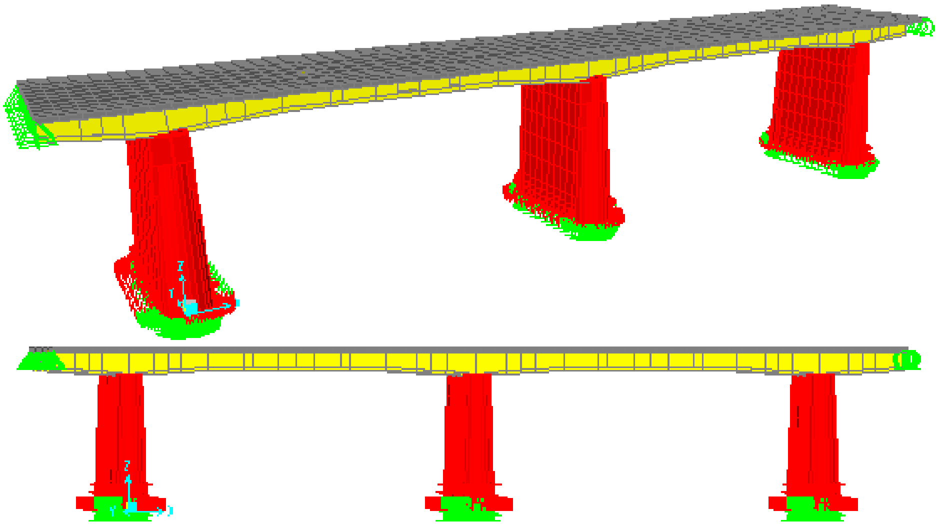

Fig. 2 Three dimensional initial finite element model of the bridge beam

The first four mode shapes obtained from analytical solutions of the bridge is given in Fig. 3. From the modal analysis, a total of four natural frequencies are attained analytically, which range between 5.770-9.400Hz. The analytical mode shapes can be classified into vertical, transverse and torsional modes.

4. Experimental measurements

Experimental measurements are performed to increase the knowledge and understanding of the behavior of a structure. This is accomplished by observing the response of a structure to a set of known conditions. In the experimental measurements, the response of the beam is measured by using B&K 8340 type uni-axial accelerometers. The minimum frequency span and sensitivity of these accelerometers are 0.1-1000Hz and 10v/g. The signals are acquired in the B&K 3560 type data acquisition system and then transferred into the PULSE Lapshop software (PULSE, 2006). For parameter estimation from the Ambient Vibration Survey data, the Operational Modal Analysis software is used (OMA, 2006). The view of the accelerometer location on the bridge is given in Fig. 4.

Normal traffic over the bridge was used as a source of ambient vibration during the tests. Since input force was not measured, the use of Operational Modal Analysis to identify modal parameters was indispensable. Three ambient vibration tests were carried out during one hour on the bridge deck. Due to the limited availability of accelerometers and data acquisition equipment, maximum 11 accelerometers for each test step could be monitored simultaneously. Among these accelerometers, a uni-axial was used as reference accelerometer and its location unchanged throughout the test. The others were used as roving accelerometers and were moved in order to cover all accelerometer locations at the vertical and transverse directions. To determine the experimental measurement tests parameters such as accelerometer numbers, points, frequency

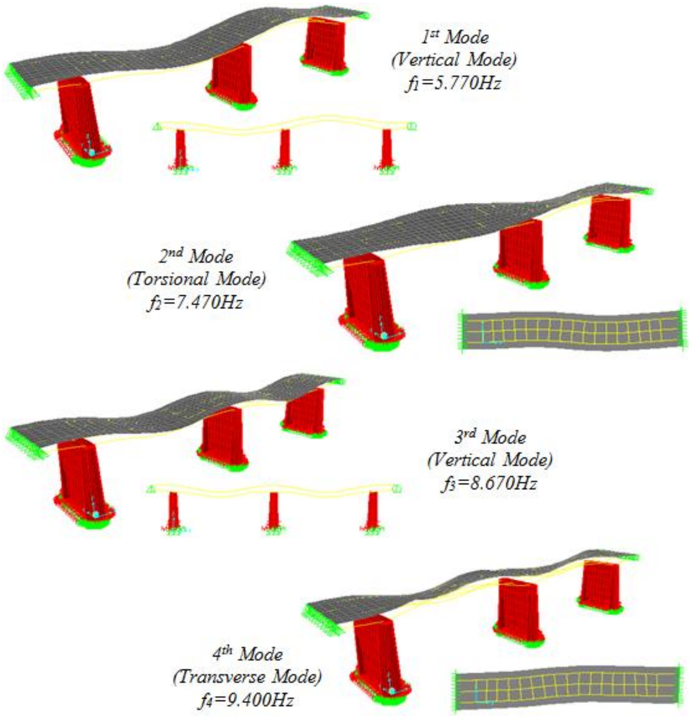

Fig. 3 Analytically identified the first four mode shapes

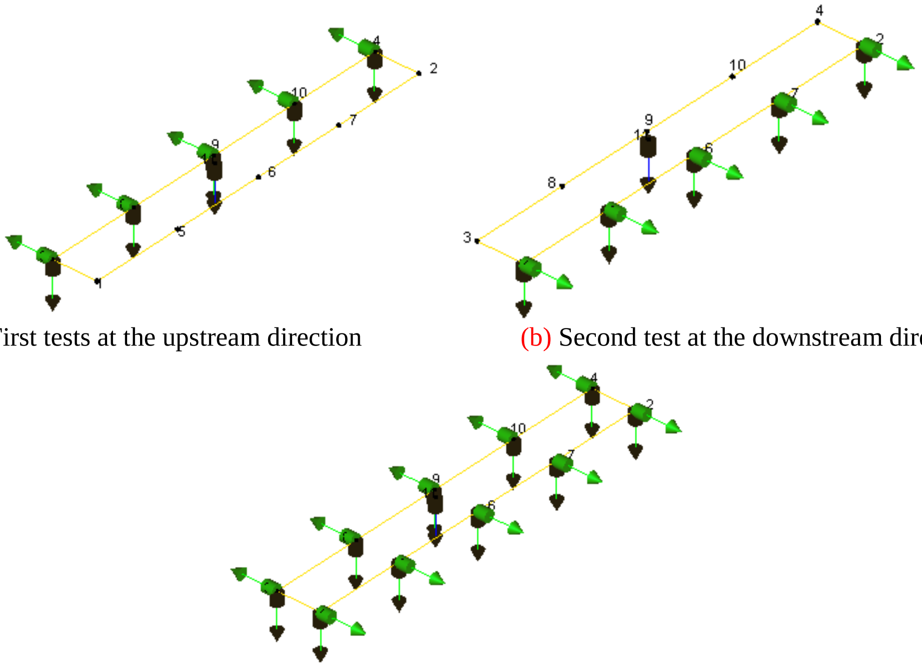

(a) First tests at the upstream direction

(b) Second test at the downstream direction

(c) Third test at the all direction

Fig. 5 The accelerometer locations for each experimental measurement

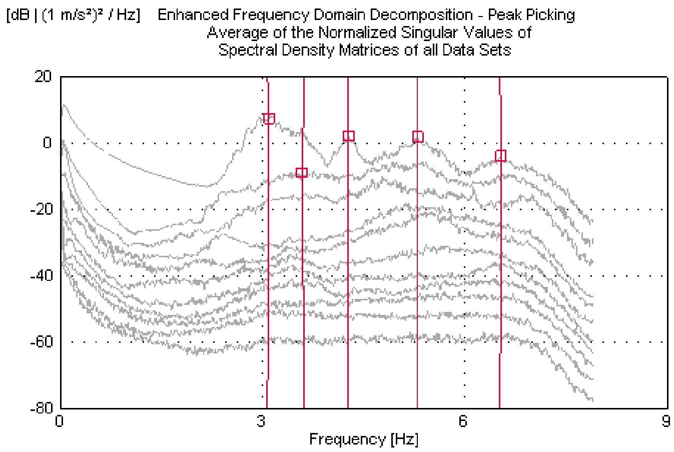

Fig. 6 Singular values of spectral density matrices

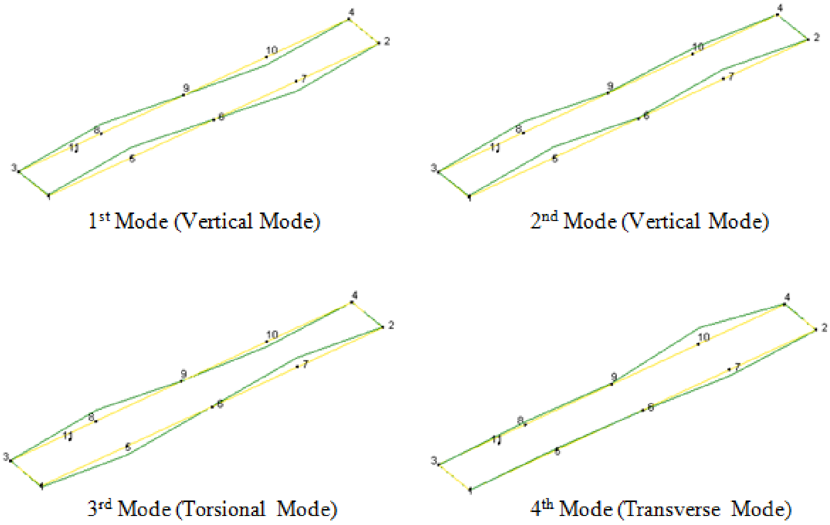

Fig. 7 Experimentally identified first four mode shapes

Table 2 Comparison of the analytical and experimental dynamic characteristics

Mod Number	Natural Frequency (Hz) *Analytical*	Natural Frequency (Hz) *Experimental*	Differences (%)	Damping Ratios (%)
1	5.770	3.078	46.7	8.046
2	7.470	4.265	42.9	2.078
3	8.670	5.287	39.0	1.453
4	9.400	6.530	30.5	0.783

span, durations etc, the initial finite element analyses results are examined and probable mode movements are evaluated. Explanation of the selected measurements points are given in Fig. 5.

Singular values of spectral density matrices of the third test setup attained from vibration signals using EFDD method are shown in Fig. 6. The first four mode shapes obtained from the experimental measurements is given in Fig. 7. When the experimentally identified mode shaped compared with each other, it is seen that there is a good agreement between all results. So, only one measurement mode shapes are given with detail in Fig. 7.

Analytically and experimentally identified dynamic characteristics of the bridge are given in Table 2. When Fig. 3, Fig. 7 and Table 2 are compared with each other, it is seen that there is some differences between mode shapes and natural frequencies. The differences in the natural frequencies are obtained between %30.5 and %46.7.

5. Finite element model updating

When the analytically and experimentally identified dynamic characteristics are compared with each other, it is seen that there is some differences between mode shapes and natural frequencies. So, finite element model of the bridge must be updated by changing of some uncertain parameters to eliminate these differences. Some deterioration was observed during field investigations on the bridge such as: regional cracks at the columns and beams, deteriorations at the supports and expansion joints, ground filling and vegetation, moisture, humidity and water infiltration and shell concrete failures due to the corrosions at some sections. Some views of the deteriorations explained in above can be seen in Fig. 8. According to these reasons, structural properties of all damaged sections were reduced. Also, semi rigid connections were designated at the foundations and expansion joints.

Comparison of the analytical and experimental dynamic characteristics of the bridge after finite element model updating is given in Table 3. According to Table 3, it is seen that maximum differences in the natural frequencies are reduced averagely from %46.7 to %2.39 and a good agreement is found between natural frequencies and mode shapes after model updating.

From the modal analysis of updated finite element model, a total of four natural frequencies are attained analytically, which range between 3.000-6.690Hz. The first analytical four mode shapes obtained from analytical solutions after model updating can be classified into vertical, transverse and torsional modes. There is a good agreement is found between mode shapes after finite element model updating. Its mean that updated finite element model reflect the current behavior of Birecik long span concrete highway bridge more accurately.

The Birecik long span concrete highway bridge consists of fourteen spans. The regions between fourteen spans were projected using expansion joint deck elements. The initial finite element analyses and experimental measurements were conducted on one span to reduce the difficulties. After the comparison of the results, finite element model of the bridge (one span) was updated.

After, the whole of the beam compartment of the bridge is constituted using updated finite element model of the one beam. Finite element model of the Birecik Highway Bridge can be seen in Fig. 9. In the finite element model, soil-structure interaction is taken into account to determine the static and dynamic behavior of the bridge more accurately.

Table 3 Analytical and experimental dynamic characteristics after model updating

Mod Number	Natural Frequency (Hz) *Analytical*	*Experimental*	Differences (%)	Damping Ratios (%)
1	3.000	3.078	2.53	8.046
2	4.920	4.265	13.3	2.078
3	4.540	5.287	14.1	1.453
4	6.690	6.530	2.39	0.783

a) Ground filling and vegetation at the columns

b) Regional cracks at the beams and columns

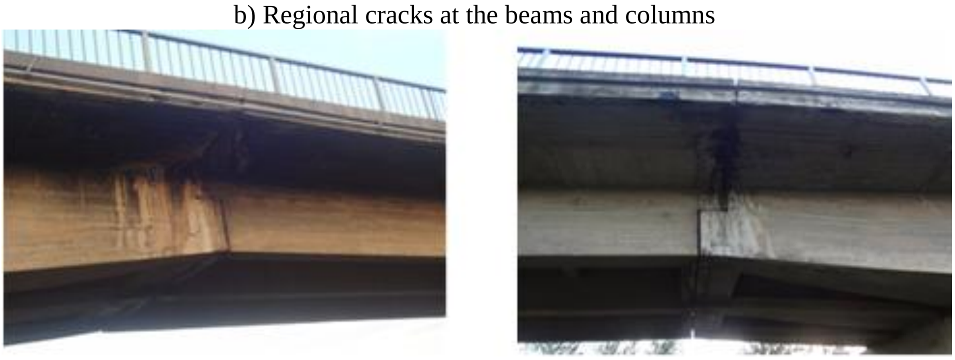

c) Moisture, humidity and water infiltration

Fig. 8 Some views of the deteriorations obtained from the field investigation

6. Structural performance evaluation

Finite element analyses are carried out to determine and compare the structural performance of the highway bridge before and after model updating. Finite element models of the bridge before and after model updating are constituted using SAP2000 software. The responses of the bridge are attained under deal loads, live loads and dynamic loads.

6.1. Structural performance of the bridge before finite element model updating

To determine the structural performance of the Birecik long span concrete highway bridge, displacements, internal forces (shear forces and bending moments) and stresses are selected as comparison parameters. The maximum vertical displacements of the bridge before model updating under dead load are shown in Fig. 10. It is seen from the Fig. 10 that displacements have an increasing trend along to the middle points of the beams. The maximum displacements are attained as 9.75mm at the spans where expansion joints exist. Also, vibrations and concussions were observed on these points by passing of heavy vehicles during experimental measurements and field investigations. Finite element analyses results clearly revealed this event. Distribution of maximum internal forces such as shear forces and bending moments, and compressive strengths before model updating under dead load are given in Fig. 11. It is seen from the Fig. 11 that maximum compressive strengths are obtained on the columns as 6MPa, maximum shear forces and bending moments taken placed on the beams which carry the deck elements as 931kNm and 480kN, and maximum compressive strengths of the deck concrete are attained as 9MPa at the expansion joints, respectively.

The maximum vertical displacements of the bridge before model updating under increased live loads are shown in Fig.12. It is seen from the Fig. 12 that displacements have an increasing

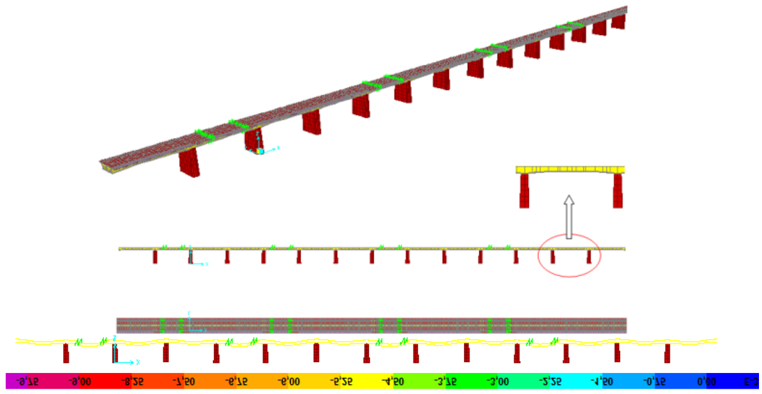

Fig. 10 The maximum vertical displacements of the bridge before model updating under dead load

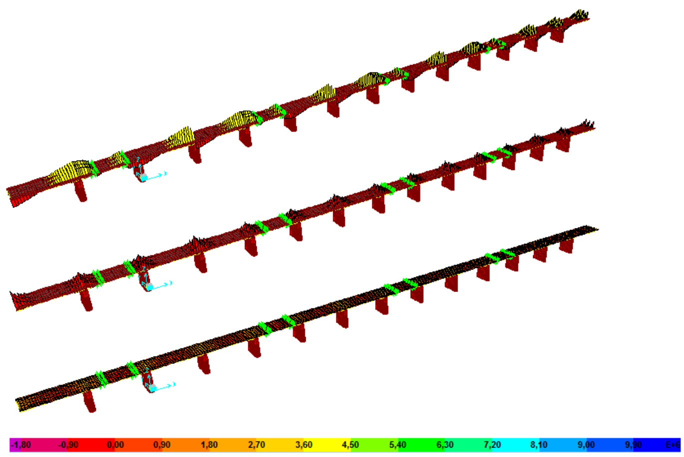

Fig. 11 Distribution of maximum internal forces and stresses before model updating under dead load

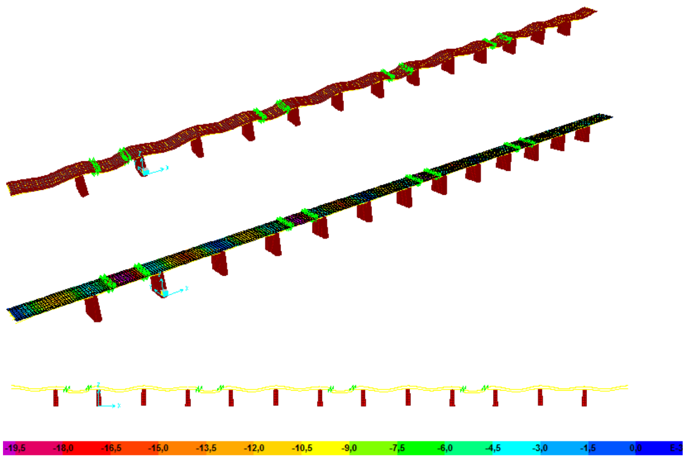

Fig. 12 The maximum vertical displacements of the bridge before model updating under increased live load

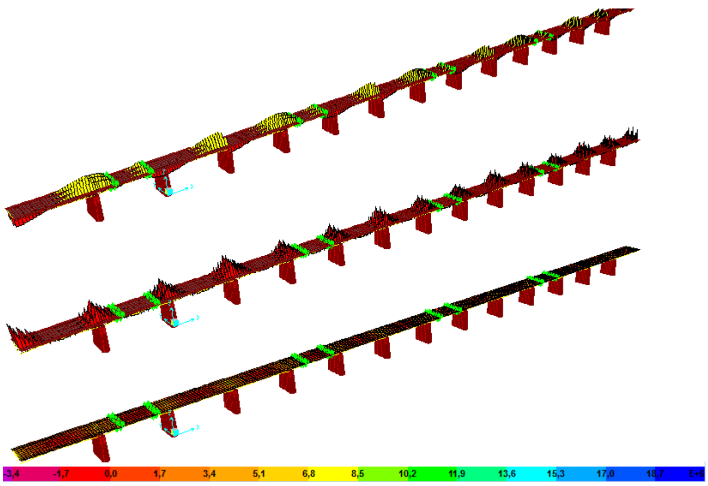

Fig. 13 Distribution of maximum internal forces and stresses before model updating under increased live load

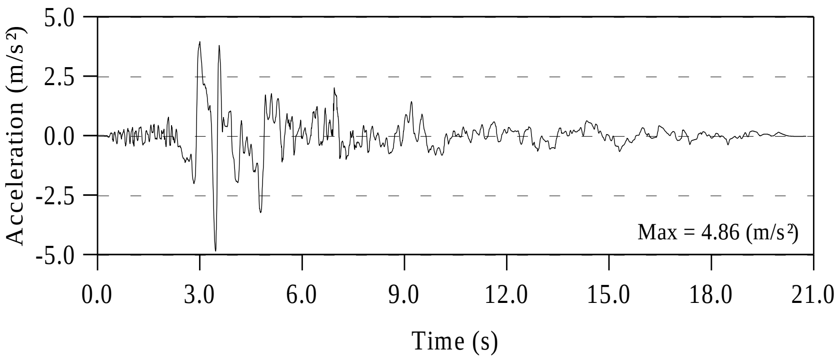

Fig. 14 Time history of ground motion acceleration of 1992 Erzincan earthquake

trend along to the middle points of the beams. The maximum displacements are attained as 19.50mm at the spans where expansion joints exist. Distribution of maximum internal forces such as shear forces and bending moments, and compressive strengths before model updating under increased live loads are given in Fig. 13. It is seen from the Fig. 13 that maximum compressive strengths are obtained on the columns as 9.5MPa, maximum shear forces and bending moments taken placed on the beams which carry the deck elements as 1500kNm and 780kN, and maximum compressive strengths of the deck concrete are attained as 14MPa at the expansion joints, respectively.

Earthquake behavior of Birecik long span concrete highway bridge before finite element model updating is performed using ERZ/EW component of 1992 Erzincan earthquake ground motion (Fig. 14). This earthquake occurred near the bridge region and has a magnitude value as 6.9 (M=6.9). The maximum vertical displacements of the bridge before model updating under dynamic loads are shown in Fig. 15. It is seen from the Fig. 15 that displacements have an increasing trend along to the middle points of the beams. The maximum displacements are attained as 24.50mm at the spans where expansion joints exist ignoring the dead and live loads.

Distribution of maximum internal forces such as shear forces and bending moments, and compressive strengths before model updating under dynamic loads are given in Fig. 16. It is seen from the Fig. 16 that maximum compressive strengths are obtained on the columns as 12.0MPa, maximum shear forces and bending moments taken placed on the beams which carry the deck elements as 2100kNm and 1000kN, and maximum compressive strengths of the deck concrete are attained as 16.5MPa at the expansion joints, respectively.

6.2 Structural performance of the bridge after finite element model updating

To determine and compare the structural performance of the Birecik highway bridge, displacements, internal forces (shear forces and bending moments) and stresses are selected as comparison parameters. The maximum vertical displacements of the bridge after model updating under dead load are shown in Fig.17. It is seen from the Fig. 17 that displacements have an increasing trend along to the middle points of the beams. The maximum displacements are attained as 8.45mm at the spans where expansion joints exist. Distribution of maximum internal forces such as shear forces and bending moments, and compressive strengths after model updating under dead load are given in Fig. 18. It is seen from the Fig. 18 that maximum compressive strengths are obtained on the columns as 4MPa, maximum shear forces and bending moments taken placed on the beams which carry the deck elements as 752kNm and 410kN, and maximum compressive strengths of the deck concrete are attained as 7.2MPa at the expansion joints, respectively.

The maximum vertical displacements of the bridge after model updating under increased live loads are shown in Fig. 19. It is seen from the Fig. 19 that displacements have an increasing trend along to the middle points of the beams. The maximum displacements are attained as 15.20mm at the spans where expansion joints exist. Distribution of maximum internal forces such as shear forces and bending moments, and compressive strengths after model updating under increased live loads are given in Fig. 20. It is seen from the Fig. 20 that maximum compressive strengths are obtained on the columns as 8MPa, maximum shear forces and bending moments taken placed on the beams which carry the deck elements as 1230kNm and 640kN, and maximum compressive strengths of the deck concrete are attained as 11.6MPa at the expansion joints, respectively.

The maximum vertical displacements of the bridge after model updating under dynamic loads are shown in Fig. 21. The maximum displacements are attained as 17.5mm ignoring the dead and live loads. Distribution of maximum internal forces such as shear forces and bending moments, and compressive strengths before model updating under dynamic loads (ignoring the dead and live loads) are given in Fig. 22. It is seen from the Fig. 22 that maximum compressive strengths are obtained on the columns as 10.2MPa, maximum shear forces and bending moments taken placed on the beams which carry the deck elements as 1720kNm and 790kN, and maximum compressive strengths of the deck concrete are attained as 13.3MPa at the expansion joints, respectively.

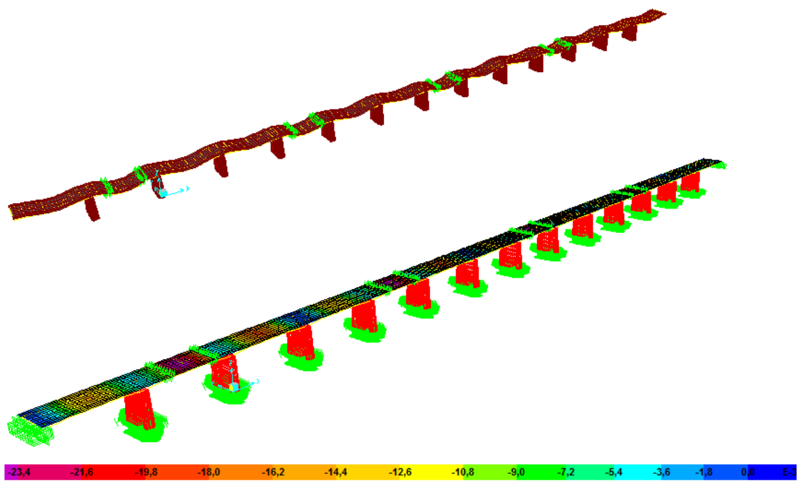

Fig. 15 The maximum vertical displacements of the bridge before model updating under dynamic load

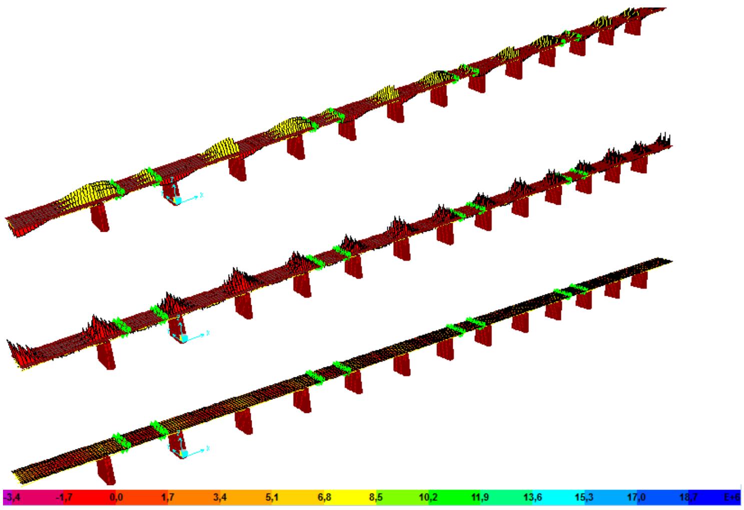

Fig. 16 Distribution of maximum internal forces and stresses before model updating under dynamic load

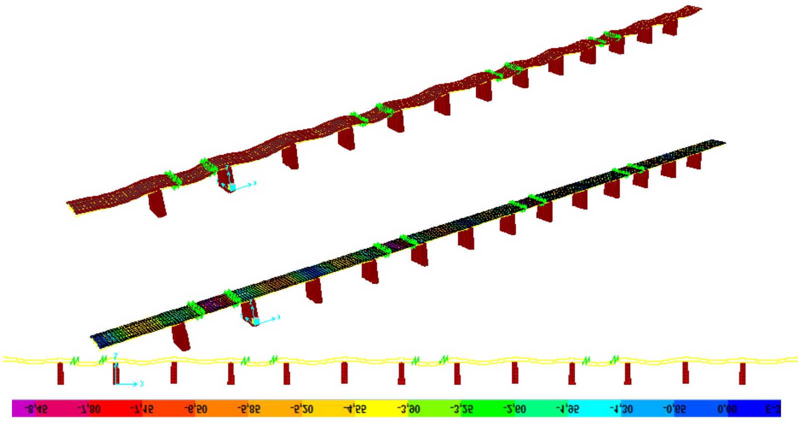

Fig. 17 The maximum vertical displacements of the bridge after model updating under dead load

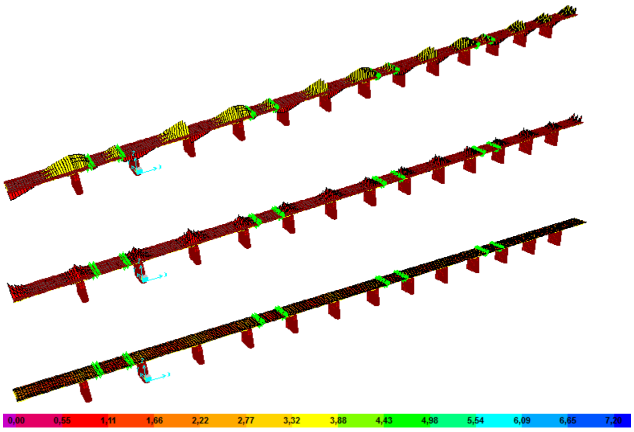

Fig. 18 Distribution of maximum internal forces and stresses after model updating under dead load

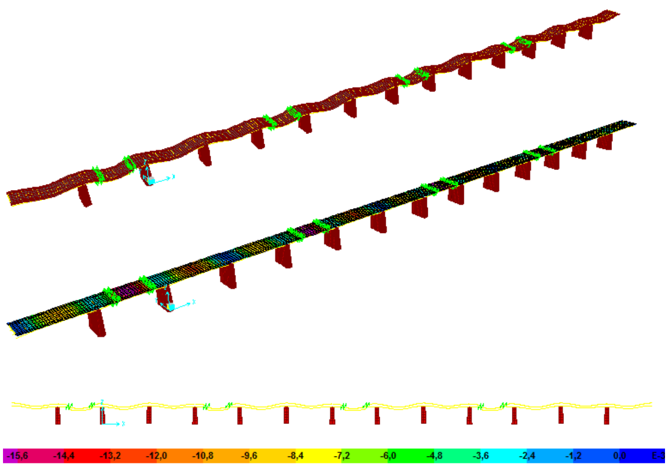

Fig. 19 The maximum vertical displacements of the bridge after model updating under increased live load

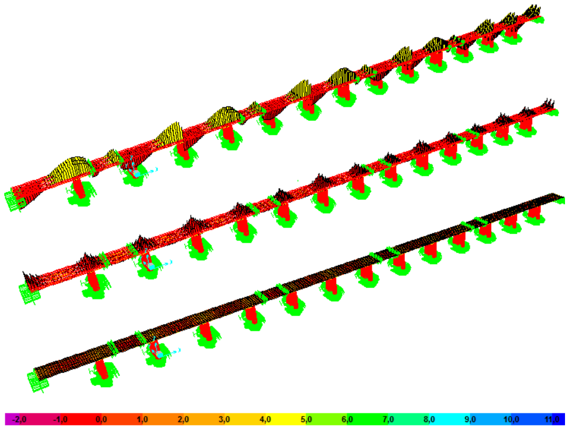

Fig. 20 Distribution of maximum internal forces and stresses after model updating under increased live load

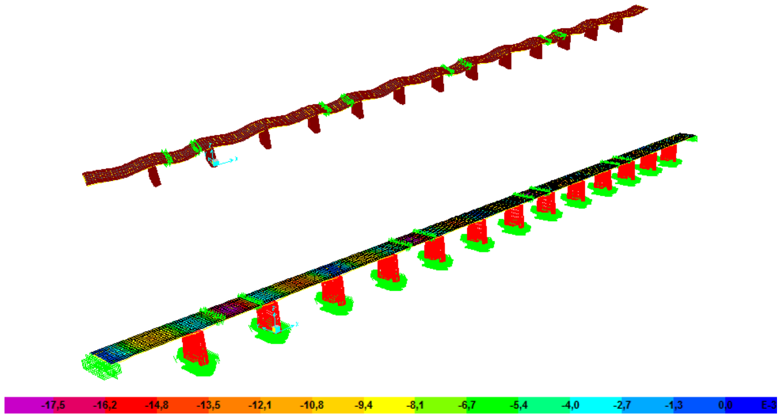

Fig. 21 The maximum vertical displacements of the bridge after model updating under dynamic load

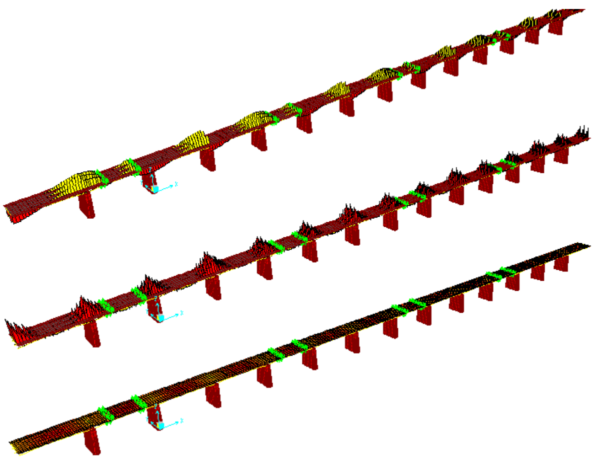

Fig. 22 Distribution of maximum internal forces and stresses after model updating under dynamic load

Table 4 Displacements, internal forces and stresses obtained before model updating

Analyses results		Analyses cases		
		Before model updating		
		*DL**	*DL**+*LL**	*DL**+*LL**+*DYL**
Displacements		9.75 mm	19.50 mm	24.50 mm
Internal Forces	*Shear Forces*	480 kN	780 kN	1000 kN
	Bending Moments	931 kNm	1500 kNm	2100 kNm
Compressive Stress	*Columns*	6.0 MPa	9.5 MPa	12.0 MPa
	Deck	9.0 MPa	14.0 MPa	16.5 MPa

*DL: Dead load *LL: Live Load *DYL: Dynamic load

Table 5 Displacements, internal forces and stresses obtained after model updating

Analyses results		Analyses cases		
		Before model updating		
		*DL**	*DL**+*LL**	*DL**+*LL**+*DYL**
Displacements		8.45 mm	15.20 mm	17.50 mm
Internal Forces	*Shear Forces*	410 kN	640 kN	790 kN
	Bending Moments	752 kNm	1230 kNm	1720 kNm
Compressive Stress	*Columns*	4.0 MPa	8.0 MPa	10.2 MPa
	Deck	7.2 MPa	11.6 MPa	13.3 MPa

*DL: Dead load *LL: Live Load *DYL: Dynamic load

The analyses results obtained from before and after finite element model updating of long span concrete highway bridge are summarized in Tables 4 and 5. According to the comparison of Tables 4 and 5, it is seen that maximum displacements are reduced averagely %13.30, %22.1 and %28.6 after finite element model updating for dead load, live load and dynamic load, respectively. Shear forces are reduced averagely %14.60, %18.0 and %21.0 after finite element model updating for dead load, live load and dynamic load, respectively. Bending moments are reduced averagely %19.22, %18.00 and %18.10 after finite element model updating for dead load, live load and dynamic load, respectively. Compressive stresses are reduced averagely %33.30, %17.80 and %15.00 for columns, %20.0, %17.15 and %19.40 for deck after finite element model updating for dead load, live load and dynamic load, respectively.

7. Conclusions

This paper presents finite element model updating effects on the structural behavior of long span concrete highway bridges. Birecik Highway Bridge located on the Şanlıurfa-Gaziantep state highway in Turkey is selected as a case study. Analytical dynamic characteristics are attained from finite element analyses using SAP2000 program. EFDD method in the frequency domain is used to extract the experimental dynamic characteristics. Finite element model of the bridge is updated to reduce the differences by changing of some uncertain parameters such as section properties, damages, boundary conditions and material properties. structural performance of the highway bridge is determined under dead load, live load, and dynamic loads before and after model updating to specify the updating effect. Comparing the results of this study, the following observations can be made:

- Initial analytical natural frequencies of Birecik long span concrete highway bridge were attained at ranges between 5.770-9.400Hz for the first four modes. These can be classified into vertical modes in the z direction, transverse modes in the y direction and torsional mode.
- The ambient vibration tests were conducted under the environmental excitations on the bridge deck for accurately extracting the dynamic characteristics using EFDD method. Three different measurement test setup were generated. According to the measurement results, it was seen that good agreement between the dynamic characteristics such as natural frequency, mode shapes and damping ratios. The first four experimental modes were estimated within ranges between 3.078-6.530Hz. These can be classified into vertical modes in the z direction, transverse modes in the y direction and torsional mode.
- When the analytically and experimentally identified dynamic characteristics of the bridge were compared with each other, it was seen that there was some differences between mode shapes and natural frequencies. The differences in the natural frequencies were obtained between %30.5 and %46.7.
- Finite element model of the bridge was updated to eliminate these differences by changing of some uncertain parameters such as regional cracks at the beams and columns, deteriorations at the supports and expansion joints, ground filling and vegetation, moisture, humidity and water infiltration, shell concrete failures due to the corrosions at some sections
- When the analytically and experimentally identified dynamic characteristics of the bridge after model updating were compared with each other, it was seen that there was a good agreement between mode shapes and natural frequencies. The differences in the natural frequencies were reduced averagely from %46.7 to %2.39.
- Finite element analyses are carried out under dead load, live load and dynamic load to determine and compare the structural performance of the highway bridge before and after model updating.

Before Finite Element Model Updating

- Displacements have an increasing trend along to the middle points of the beams. The maximum displacements are attained as 9.75mm at the spans where expansion joints exist. Also, vibrations and concussions were observed on these points by passing of heavy vehicles during experimental measurements and field investigations. Finite element analyses results clearly revealed this event. Maximum compressive strengths are obtained on the columns as 6MPa, maximum shear forces and bending moments taken placed on the beams which carry the deck elements as 931kNm and 480kN, and maximum compressive strengths of the deck concrete are attained as 9MPa at the expansion joints, respectively.
- Displacements have an increasing trend along to the middle points of the beams. The maximum displacements are attained as 19.50mm at the spans where expansion joints exist. Maximum compressive strengths are obtained on the columns as 9.5MPa, maximum shear forces

and bending moments taken placed on the beams which carry the deck elements as 1500kNm and 780kN, and maximum compressive strengths of the deck concrete are attained as 14MPa at the expansion joints, respectively.

- Displacements have an increasing trend along to the middle points of the beams. The maximum displacements are attained as 24.50mm at the spans where expansion joints exist ignoring the dead and live loads. Maximum compressive strengths are obtained on the columns as 12.0MPa, maximum shear forces and bending moments taken placed on the beams which carry the deck elements as 2100kNm and 1000kN, and maximum compressive strengths of the deck concrete are attained as 16.5MPa at the expansion joints, respectively.

After Finite Element Model Updating

- Displacements have an increasing trend along to the middle points of the beams. The maximum displacements are attained as 8.45mm at the spans where expansion joints exist. Maximum compressive strengths are obtained on the columns as 4MPa, maximum shear forces and bending moments taken placed on the beams which carry the deck elements as 752kNm and 410kN, and maximum compressive strengths of the deck concrete are attained as 7.2MPa at the expansion joints, respectively.
- Displacements have an increasing trend along to the middle points of the beams. The maximum displacements are attained as 15.20mm at the spans where expansion joints exist. Maximum compressive strengths are obtained on the columns as 8MPa, maximum shear forces and bending moments taken placed on the beams which carry the deck elements as 1230kNm and 640kN, and maximum compressive strengths of the deck concrete are attained as 11.6MPa at the expansion joints, respectively.
- The maximum displacements are attained as 17.5mm ignoring the dead and live loads. Maximum compressive strengths are obtained on the columns as 10.2MPa, maximum shear forces and bending moments taken placed on the beams which carry the deck elements as 1720kNm and 790kN, and maximum compressive strengths of the deck concrete are attained as 13.3MPa at the expansion joints, respectively.

❖ According to the comparison of analyses results, it is seen that maximum displacements are reduced averagely %13.30, %22.1 and %28.6 after finite element model updating for dead load, live load and dynamic load, respectively.

❖ Shear forces are reduced averagely %14.60, %18.0 and %21.0 after finite element model updating for dead load, live load and dynamic load, respectively.

❖ Bending moments are reduced averagely %19.22, %18.00 and %18.10 after finite element model updating for dead load, live load and dynamic load, respectively.

❖ Compressive stresses are reduced averagely %33.30, %17.80 and %15.00 for columns, %20.0, %17.15 and %19.40 for deck after finite element model updating for dead load, live load and dynamic load, respectively.

Acknowledgements

This research was supported by TUBITAK and Karadeniz Technical University (KTU) under Research Grant No. 106M038, 2006.112.001.1, respectively. Also, many thanks to Assistant Professor Temel Türker to his help in the experimental measurements of the bridge.

References

Ansari, F. (1987), "Stress-strain response of microcracked concrete in direct tension", *ACI Mater. J.*, **84**(6), 481-490.

Bagheripour, M.H., Rahgozar, R., Pashnesaz, H. and Malekinejad, M. (2011), "A complement to hoek-brown failure criterion for strength prediction in anisotropic rock", *Geomech. Eng.*, **3**(1), 61-81.

Balmer (1949), *Shearing Strength of Concrete under High Triaxial Stress—Computation of Mohr's Envelope as a Curve*, Structural Research Laboratory Report, No SP-23, United States Department of the Interior, Bureau of Reclamation, Washington, DC.

Bhargava, P., Bhowmick, R., Sharma, U. and Kaushik, S.K. (2006), "Three-dimensional finite element modeling of confined high-strength concrete columns", *Special Publication, ACI* , **238**, 249-266.

Bortolotti, L., Carta, S. and Cireddu, D. (2005), "Unified yield criterion for masonry and concrete in multiaxial stress states", *ASCE, J. Mater. Civil Eng.*, **17**(1), 54-62.

Brestler, B. and Pister. (1958), "Behavior of concrete under triaxial compressive-compressive-tensile stresses", *ACI Mater. J.*, **8**(2), 181-185.

Brestler, B. and Pister. (1958), "Strength of concrete under combined stresses", *Proceedings of ACI Journal*, **55**(3), 321-346.

Buyukozturk, O. and Shareef. S.S. (1985), "Constitutive modeling of concrete in finite element analysis", *Comput. Struct.*, **21**(3), 581-610.

Carreira, D.J. and Chu, K.H. (1986), "Stress-strain relationship for plain concrete in compression", *Proceedings of ACI Journal*, **82**(6), 797-804.

Cedolin, L. and Mulas, M.G. (1984), "Biaxial stress-strain relation for concrete", *ASCE, J. Eng. Mech. Div.*, **110**(2), 187-206.

Cedolin, L., Crutzen, Y.R.J. and Dei Poli, S. (1977), "Triaxial stress-strain relationship for concrete", *ASCE, J. Eng. Mech. Div.*, **103**(3), 423-439.

Chen, A.C.T. and Chen, W.F. (1975), "Constitutive relations for concrete", *J. Eng. Mech. Div.* **101**(4), 465-481.

Chen, W. F. (1982), "Plasticity in reinforced concrete", McGraw-Hill, New York.

Chen, W.F. and Han, D.J. (2008), "Plasticity for structural engineers", *J. Ross Publishing*, India.

Darwin, D. and Pecknold, D.A. (1977), "Nonlinear biaxial stress-strain law for concrete", *ASCE, J. Eng. Mech. Div.*, **103**(2), 229-241.

Dede, T. and Ayvaz, Y. (2010), "Comprative study of plasticity models for concrete material by using different criteria including Hseih-Ting-Chen criterion", *Mater. Des.*, **31**(3), 1482-1489.

Du, X.L., Lu D.C., Gong, Q.M. and Zhao, M. (2010), "Nonlinear unified strength criterion for concrete under three-dimensional stress states", *ASCE, J. Eng. Mech. Div.*, **131**(1), 51-59.

Fanning, P. (2001), "Nonlinear models of Reinforced and post-tensioned concrete beams", *Elect. J. Struct.*, **2**, 111-119.

Fan, S.C. and Wang, F. (2002), "A new strength criterion for concrete", *ACI Struct. J.*, **99**(3), 317-326.

Fardis, M.N., Alibe, B. and Tasoulas, J.L. (1983), "Monotonic and cyclic constitutive law for concrete", *ASCE, J. Eng. Mech. Div.*, **109**(2), 516-536.

Fehling, E., leutbecher, T. and Roeder, F.K. (2011), "Compression-Tension strength of Reinforced and Fiber-Reinforced concrete", *ACI Struct. J.*, **108**(3), 350-359.

Folino, P., Etse, G. and Will, A. (2009), "Performance dependent failure criterion for normal-and high-strength concretes", *ASCE, J. Eng.Mech. Div.*, **35**(12), 1393-1409.

Gardner, N.J. (1989), "Triaxial behavior of concrete", *Proceedings of ACI Journal*, **66**(2), 136-146.

Gopalarathnam, V.S. and Shah, S.P. 1985), "Softening response of plain concrete in direct tension", *ACI Struct. J.*, **82**(2), 310-323.

Han, D.J. and Chen, W.F. 1987), "Constitutive modelling in analysis of concrete structures", *ASCE, J. Eng. Mech. Div.*, **113**(4), 577-593.

Hinchberger, S.D. (2009), "Simple single-surface failure criterion for concrete", Technical Notes. *ASCE, J.*

Eng. Mech., **135**(7), 729-732.
Hognestad, E., Hansen, N.W. and McHenry, D. (1955), "Concrete stress distribution in ultimate strength design", *ACI Journal*, **52**(4), 455-480.
Hughes, B.P. and Chapman, G.P. (1966), "The complete stress-strain curve for concrete in direct tension", *RILEM Bulletin*, **30**, 95-97.
Hussein, A. and Marzouk, H. (2000), "Behavior of high-strength concrete under biaxial stresses", *ACI Mater. J.*, **97**(1), pp. 27-36.
Imran, I. and Pantazopoulou, S.J. (2001), "Plasticity model for concrete under triaxial compression", *ASCE, J. Eng. Mech. Div.*, **127**(3), 281-290.
Imran, I. and Pantazopoulou, S.J. (1991), "Experimental study of plain concrete under triaxial stresses", *ACI Mater. J.*, **93**(6), 589-601.
Karam, G. and Tabbara, M. (2012), "Hoek-brown strength criterion for actively confined concrete", *J. Mater. Civil Eng.*, **21**(3), 110-118.
Karsan, I.D. and Jirsa, J.O. (1969), "Behavior of concrete under compressive loadings", *ASCE, J. Struct. Div.*, **95**(12), 2543-2563.
Kotsovos, M.D. and Newman J.B. (1977), "Behavior of concrete under multiaxial stress", *Proceedings of ACI J.*, **74**(9), 443-446.
Kupfer, H. and Gerstle. (1973), "Behavior of concrete under biaxial stresses", *ASCE, J. Eng. Mech. Div.*, **99**(4), 853-866.
Kupfer, H., Hilsdorf, H.K. and Rusch, H. (1969), "Behavior of concrete under biaxial stresses", *Proceedings of ACI J.*, **66**(8), 656-666.
Kwak, H.G. and Filippou, F.P. (1990), *Finite Element Analysis of Reinforced Concrete Structures under Monotonic Loads*, Report No. UCB/SEMM-90/14, *Earthquake Engineering Research Centre*, University of California, Berkeley.
Li, L.Y. and Harmon T.G. (1990), "Three-parameter failure criterion for concrete", *ASCE, J. Mater. Civil Eng.*, **2**(4), 215-222.
Lan, S. and Guo, Z. (1999), "Biaxial compression behavior of concrete under repeated loading", *ASCE, J. Mater. Civil Eng.*, **105**(11), 105-115.
Lee, S.K., Song, Y.C. and Han, S.H. (2004), "Biaxial behavior of plain concrete of nuclear containment building", *Nuclear Eng. Des.*, **227**(2), 143-153.
Linhua, J., Dahai, H. and Nianxiang, X. (1991), "Behavior of concrete under triaxial compressive-compressive tensile stresses", *ACI Mater. J.*, **88**(2), 181-185.
Liu, T.C.Y., Nilson, A.H. and Slate, S.F.O. (1972), "Stress-strain response and fracture of a concrete in uniaxial and biaxial compression", *Proceedings of ACI Journal*, **69**(5), 291-295.
Menetrey, P. and Willam, K.J. (1995), "Triaxial failure criterion for concrete and its generalization", *Proceedings of ACI Journal*, **92**(3), 311-318.
Mills, L.L. and Zimmerman, R.M. (1970), "Compressive Strength of Plain Concrete Under Multiaxial Loading Conditions", *Proceedings of ACI J.*, **67**(10), 802-807.
Mlakar, P.F., Vitaya-Udom, K.P. and Cole, R.A. (1985), "Dynamic tensile-compressive behavior of concrete", *ACI Journal*, **86**(5), 484-491.
Mansour, M.H. (2010), "Theoretical analysis of tunnel lining subjected to fire", *J. Eng. Sci.*, **38**(3), 619-640.
Nayak, G.C. and Zeinkiewicz, O.C. (1972), "Convenient forms of stress invariants for plasticity", *ASCE, J. Struct. Eng.*, **98**(4), 949-954.
Ottosen N.S. (1993), "A failure criterion for concrete", *ASCE, J. Eng. Mech. Div.*, **103**(4), 527-535.
Ren, X., Yang, W., Zhou, Y. and Li, J. (2008), "Behavior of high performance concrete under uniaxial and biaxial loading", *ACI Mater. J.*, **105**(6), 548-557.
Ribeiro, G. de O. and Oliveira, A.L. (1998), "Elastoplastic analysis of RC plates using the Reissner's model and the boundary element method", *Proceedings of Computational Mechanics, New Trends and Applications*, Barcelona, Spain.
Seow, P.E.C. (2005), "A unified failure criterion for normal, high-strength and steel fibre-reinforced concrete", PhD Thesis, Department of Civil Engineering, National University of Singapore, Singapore.

Seow, P.E.C. and Swaddiwudhipong S. (2005), "Failure surface for concrete under multiaxial load - a unified approach", *ASCE*, *J. Mater.Civil Eng*., **17**(2), 219-228.
Sinha, B.P., Gerstle, K.H. and Tulin, L.G.(1964), "Stress-strain relations for concrete under cyclic loading", *Proceedings of ACI Journal*, **61**(2), 195-212.
Tasuji, M.E., Slate, F.O. and Nilson, A.H. (1978), "Stress-strain response and fracture of concrete in biaxial loading", *Proceedings of ACI Journal*, **75**(7), 306-312.
Tsai, W.T. (1988), "Uniaxial compressional stress-strain relation of concrete", *ASCE*, *J. Struct. Div*., *ASCE*, **114**(9), 2133-2166.
Vecchio (1998), "Lessons from the analysis of a 3-D concrete shear wall", *Struct. Eng. Mech*., **6**(4), 439-455.
Willam, K. and Warnke, E. (1975), "Constitutive model for triaxial behaviour of concrete", *Proceedings of the International Association for Bridge and Structural Engineering*, Zurich, Switzerland, 1-30.
Yan, Z. and Pantelides, C.P. (2006), "Fiber-Reinforced polymer jacketed and shape - modified compression members: II – Model", *ACI Struct. J*., **103**(6), 894-903.
Yin, W.S., Su, E.C.M., Mansur, M.A. and Hsu, T.T.C. (1989), "Biaxial tests of plain and fibre concrete", *ACI Mater. J*., **86**(3), 236-243.
Yu, M.H. (2002b), "Advances in strength theories for materials under complex stress state in the 20th century", *Appl. Mech. Rev. ASME*, **55**(3), 169-218.
Yu, M.H. (2004), "Unified strength theory and its applications", *Springer*, *Berlin*.
Zhi, W.C., Hai, G.Z. and Qin, Z.X. (1987), "Experimental investigation of biaxial and triaxial compressive concrete strength", *ACI Mater. J*., **84**(2), 92-100.

CC